Lineage structure of *Streptococcus pneumoniae* is driven by immune selection on the groEL heat-shock protein.

José Lourenço[1,*], Eleanor R. Watkins[1], Uri Obolski[1], Samuel J. Peacock[1], Callum Morris[2], Martin C. J. Maiden[1], and Sunetra Gupta[1]

[1]Department of Zoology, University of Oxford, Oxford, United Kingdom
[2]University of Durham, Durham, United Kingdom
[*]jose.lourenco@zoo.ox.ac.uk

ABSTRACT

Populations of *Streptococcus pneumoniae* (SP) are typically structured into groups of closely related organisms or lineages, but it is not clear whether they are maintained by selection or neutral processes. Here, we attempt to address this question by applying a machine learning technique to SP whole genomes. Our results indicate that lineages evolved through immune selection on the groEL chaperone protein. The groEL protein is part of the *groESL* operon and enables a large range of proteins to fold correctly within the physical environment of the nasopharynx, thereby explaining why lineage structure is so stable within SP despite high levels of genetic transfer. SP is also antigenically diverse, exhibiting a variety of distinct capsular serotypes. Associations exist between lineage and capsular serotype but these can be easily perturbed, such as by vaccination. Overall, our analyses indicate that the evolution of SP can be conceptualized as the rearrangement of modular functional units occurring on several different timescales under different pressures: some patterns have locked in early (such as the epistatic interactions between *groESL* and a constellation of other genes) and preserve the differentiation of lineages, while others (such as the associations between capsular serotype and lineage) remain in continuous flux.

Introduction

Streptococcus pneumoniae (the pneumococcus) is a gram-positive bacterial pathogen which, although commonly carried asymptomatically in the nasopharynx, can cause pneumonia, meningitis, septicemia and bacteremia in the young, elderly and immuno-compromised, being responsible for about 11% of worldwide deaths in children under 5 years of age[1,2]. Populations of *S. pneumoniae* are antigenically diverse and can be stratified into more than 90 serotypes according to the antigenic properties of the expressed polysaccharide capsule, of which only 10-15 are responsible for most cases of invasive disease worldwide[3]. Reductions in disease rates have been achieved by the deployment of the PCV7 vaccine targeting 7 of the most common serotypes in invasive disease, and more recently through the use of PCV13 which extends coverage to an additional 6 serotypes. However this has been accompanied by an increase in the frequency of non-vaccine serotypes in many parts of the world, likely due to the removal of competition from vaccine serotypes[4].

Like many other bacterial pathogen populations, *S. pneumoniae* may be organised into a number of so-called clonal complexes on the basis of allelic diversity at selected housekeeping loci (determining Multilocus Sequence Type,[5,6]). Pneumococcal populations are also structured at a whole genome level into co-circulating lineages or Sequence Clusters (SC) bearing unique signatures of alleles[7–9]. The relationships between clonal complex, lineage and serotype are often found to be non-overlapping[8,10], although subject to perturbations such as through vaccination[11].

The maintenance of discrete major lineages, and their associations with distinct serotypes and clonal complexes, is hard to ascribe to purely neutral processes, given the high rate of genetic exchange in these pathogen populations[12,13]. We have previously proposed that extensive co-adaptation between loci may give rise to these patterns, as even small fitness differences among different combinations of alleles can lead to the loss of less fit genotypes under intense competition for resources[14]. Bacterial populations could also segregate into a set of successful *metabolic types* which are able to co-circulate by virtue of exploiting separate metabolic niches and thereby avoiding direct resource competition[15]. As an example, specific differences in the ability to absorb particular carbohydrate resources have been observed in functional genomics studies of *S. pneumoniae*[16], and these may reflect specialization upon different resources within the same environment as a means of avoiding competition. Establishing the contribution of co-adaptation and competition in the maintenance of discrete lineages is important since the outcome of certain interventions, such as vaccination, depends crucially on these underlying determinants of population structure[17].

Here, we attempt to elucidate potential drivers of lineage structure by applying a machine learning technique known as the Random Forest Algorithm (RFA) to a dataset containing 616 whole genomes of *S. pneumoniae* collected in Massachusetts (USA) between 2001 and 2007[8]. RFA-based methods have been robustly applied in genome-wide association studies of cancer and chronic disease risk[18], species classification[19], or in the search of viral determinants for host tropism, for instance by identifying the key amino-acid sites that determine host specificity of zoonotic viruses[20], and by selecting the clear genetic distinctions in avian and human proteins of Influenza viruses[21,22]. In the context of bacterial pathogens, these methods have been sucessfully used to analyse the genetic background of *Escherichia coli* cattle strains more likely to be virulent to humans[23], to identify *Staphylococcus aureus* genetic variants associated with antibiotic resistance[24], and to discover that repertoires of virulence proteins within different Legionella species are largely unique (non-overlapping)[25]. An RFA is an ensemble method that combines the information of multiple, regression or classification trees built around predictor variables towards a response variable. The output of an RFA is composed both of the classification success rates of the response variable and a ranking of the predictor variables quantifying their relative role in the classification process.

We used as response variables (i) the capsular serotype of each isolate (which had been determined by serological means), and (ii) the monophyletic Sequence Cluster (SC) to which samples had been assigned[8]. We set the predictor variables to be the 2135 genes for which we had obtained allelic profiles (effectively using a whole-genome multi-locus sequence typing approach[26]) for each of the 616 isolates[17]. Using this method, we confirmed that capsular genes predict serotype, but found a clear disjunction between these genes and those which predict SC (lineage). Furthermore, our analyses revealed that, contrary to the expectations of neutrality, genes which predict lineage are non-randomly distributed across the genome, clustering within and around the *groESL* operon, leading us to propose that a combination of immune selection and coadaptation operating upon these loci may be the primary determinants of lineage structure.

Results

Classification success for serotype and sequence cluster

Classification of SC by the RFA was accurate (Fig. S1B) with all SC types being predicted with success close to 100%. This is a reflection of the strong correspondence between classification trees and taxonomy when based on genetic information, as explored in other studies[19], and demonstrated by Austerlitz and colleagues when comparing the success of RFA, neighbour-joining and maximum-likelihood methodologies on simulated and empirical genetic data[27].

By contrast, the success rate in identifying the capsular serotypes of the 616 whole genomes, although also very high (above 75% for the majority of serotypes), was not perfect (Fig. S1A). This is to be expected given the imperfect association between lineage and serotype, and also because certain serotypes were represented by very small numbers of isolates (as an extreme example, only a single isolate of serotype 21 was present and therefore classification success was nil).

The capsular locus is a strong predictor of serotype but performs indifferently in predicting sequence cluster

As might be expected, genes within the capsular locus (defined as being within but not including the genes *dexB* and *aliA*) were higly predictive of serotype, with their RFA scores appearing as outliers in the top 2.5% of the distribution defined by all 2135 genes in the dataset (Fig. 1A, see Methods). However, these did not score above average in predicting SC, as their RFA scores shifted closely to the distribution's average (Fig. 1B). We noted, however, that many of these genes contained what appeared to be a high proportion of deletions but, in fact, had simply eluded allelic notation (alleles 'x', see Methods) on account of their high diversity at the level of the population (see, for example,[28]). For certain genes, such as those encoding the polysaccharide polymerase Wzy and the flippase Wzx, the allelic notation process failed at least 50% of the time for over 90% of the isolates, essentially working only for serotype 23F (the reference genome) and the closely related 23A and 23B serotypes. In general, the degree of success in allelic notation of each gene was closely linked to the potential for alignment with its counterpart in the 23F reference genome (Fig. S4). Nonetheless, the same shift towards lower RFA scores of capsule-associated genes in predicting SC rather than serotype was observed upon performing a series of sensitivity classification exercises after excluding all genes which contained $> 50\%$ (Fig. S2) or $> 10\%$ (Fig. S3) of gene mismatches/deletions. When imposing an exclusion criterion of $> 10\%$ we retained only the genes *wze*, *wzg* and *wzh* (in addition to two pseudogenes) within the capsular locus, and these could also clearly be seen to shift from above the upper 97.5% limit into the neutral expectation of RFA scores when predicting SC (Fig. S3).

We next performed the same analysis excluding all genes which showed mismatches or deletions above a threshold of 1%, in an attempt to eliminate possible biases in RFA output due residual information arising from the distribution of mismatches/deletions. This left us with 1581 genes which were shared by virtually all the samples in our dataset and for which function could be correctly ascertained by querying the reference genome. It is likely that these genes correspond to the approximately 1500 core cluster of orthologous genes (COGs) identified by Croucher *et al* in their recent analysis of the same

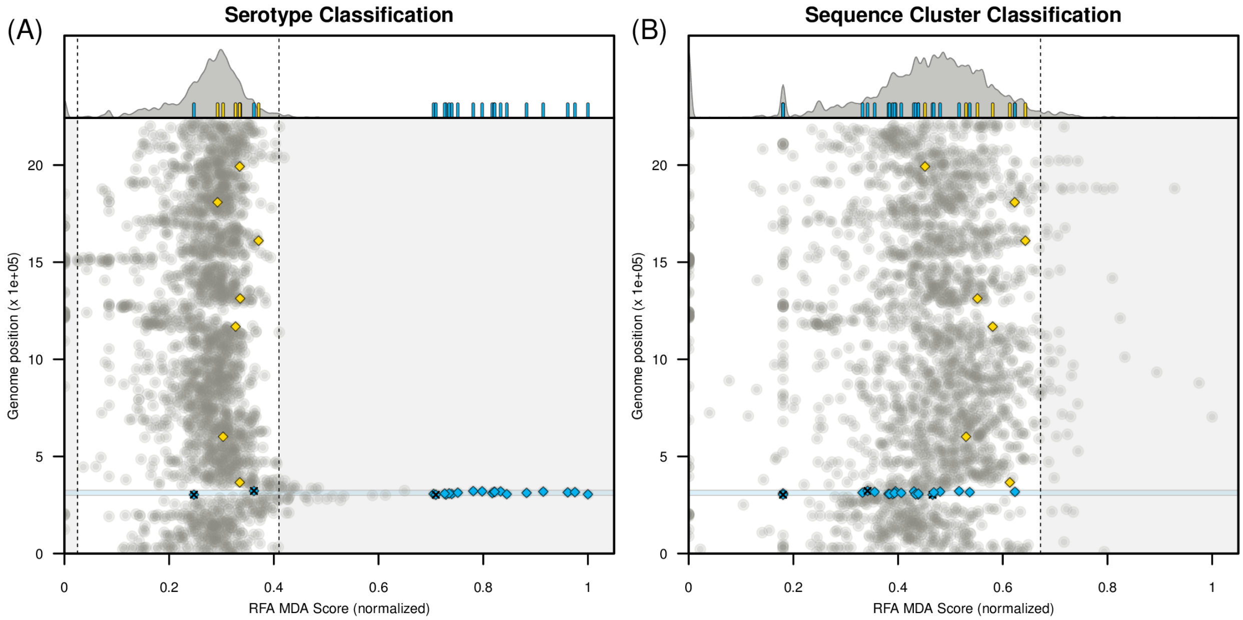

Figure 1. Random forest classification. *(A)* Random forest analysis (RFA) for serotype classification. *(A, top)* Density function of RFA scores obtained for each gene in the dataset. The 95% boundaries are marked by the dashed lines. Small bars highlight the RFA scores of genes within particular groups (yellow for MLST genes, blue for capsular locus genes). *(A, bottom)* Genomic position for each gene in the dataset against their RFA score (normalised to [0,1]). The circular genome is presented in a linear form on the y-axis, with the first gene being *dnaA* and the last gene *parB*. MLST genes are marked in yellow diamonds (*spi, xpt, glkA, aroE, ddlA, tkt*) and genes within the capsular locus with blue diamonds (pseudogenes tagged with 'x'). *(B)* RFA analysis for sequence cluster classification; figure details the same as in *A*. Blue shaded areas in both A and B subplots mark the capsular locus (genes within *aliA* and *dexB*).

dataset[7]. This approach eliminated all of the genes considered above as belonging within the capsular locus, although flanking genes were retained and a number of these achieved the top 2.5% of RFA scores in predicting serotype (Fig. 2A, Table 1): 38% of the top genes occurred within 10 genes downstream and upstream of the capsular locus, and 90% were situated within 129 genes (which amounts for 6% of the genome). The remaining 10% of top-scoring genes, *lytC*, *trpF*, *patB* and SPNF2300400 were located at significantly longer distances from the capsular locus, at 963 (45% of the genome), 710, 469 and 270 (13% of the genome) genes away, respectively. None of the genes achieving the top 2.5% of RFA scores in predicting serotype (shown in red in Fig. 2) remained in the top 2.5% category when asked to predict SC. Similarly, all genes which achieved top scores in predicting SC (Table 2) were only of average importance in elucidating serotype (shown in green in Fig. 2).

Sequence cluster is predicted by variation in the groESL operon

About 75% of top-scoring genes for SC were uniformly distributed along the genome (Fig. 2B), while the remaining 25% of the genes were contiguous and contained within the *groESL* operon, encoding the GroEL chaperone and GroES co-chaperone proteins (Table 2). Notably, other studies have reported the power of the *groESL* operon and its proteins to ascertain phylogeny and classification within the *Streptococcus* genus[29] and between species of the *Viridans* and *Mutans* Streptococci groups[30,31].

A number of other top scoring genes in predicting SC have also previously been demonstrated to be powerful discriminators of genealogy in a range of bacterial species. For instance, *sodA*, encoding for the manganese superoxide dismutase, critical against oxidative stress and linked to both survival and virulence, has been highlighted in numerous studies for its relevance in identification of rare clones of pneumococci[32,33] and Streptococci at the species level[34,35]. Another example is the *lmb* gene, encoding for an extracellular protein with a key role in physiology and pathogenicity[36,37]. Homologs of this protein have been documented to be present and discriminatory of at least 25 groups of the *Streptococcus* genus with possible similar functions[38,39].

The housekeeping genes included in multilocus sequence typing (MLST) classification performed no better than average in predicting SC across the sensitivity experiments (Fig. 1, S1-3). The exception was the Signal Peptidase I gene (*spi*), which featured in the top-scoring genes predicting SC under the strict 1% cutoff (Table 2). This is unsurprising, however, as MLST genes are unlikely to dictate lineage differentiation through selective processes, which endorses their choice as good

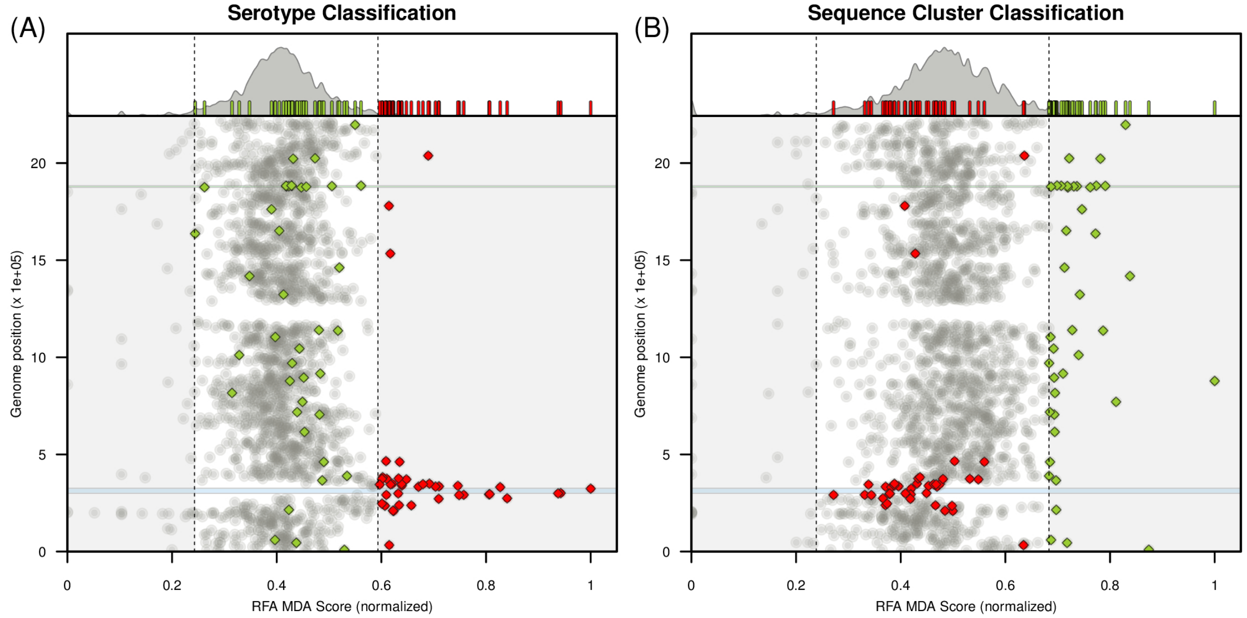

Figure 2. Random forest classification excluding data with gene mismatches. *(A)* Random forest analysis (RFA) for serotype classification when excluding genes for which the allelic notation process had $<$ 99% positive matches with the reference genome. *(A, top)* Density function of RFA scores obtained for each gene in the dataset. The 95% boundaries are marked by the dashed lines. Small bars highlight the RFA scores of genes within particular groups (red for serotype, green for SC genes). *(A, bottom)* Genomic position for each gene in the dataset against their RFA score (normalised to [0,1]). The circular genome is presented in a linear form on the y-axis, with the first gene being *dnaA* and the last gene *parB*. Red and green diamonds mark the top 2.5% ranking genes for serotype and Sequence Cluster classification, respectively. *(B)* RFA for Sequence Cluster classification; figure details the same as in *A*. Blue shaded areas in both A and B mark the capsular locus (genes within *aliA* and *dexB*). Green shaded areas in both A and B mark the genes contiguous and including the *groESL* operon (Table 1).

discriminators of recent neutral diversification, in particular within recent epidemiological events[5,6].

Top-scoring genes for serotype are associated with resource competition and antibiotic resistance

When analyzing the 39 top-scoring, non-capsular genes which were highly predictive of serotype, we found 24 (62%) with compelling support for functional background that could mediate pneumococcal competitive interactions or niche specialization, at least in related streptococcal species (reviewed in detail in supplementary text). For instance, ATP-binding cassette (ABC) transporter genes, critical for intake, antibiotic resistance and metabolism, were found 5 times more frequently in the genes predictive of serotype compared to those determining SC (Tables 1 and 2). Notably, our approach selected the genes encoding for the pit ABC transporter, a key player in iron uptake known to exhibit strain-specific variation[40], but did not select two other operons encoding iron transporters (*piu*, *pia*), which are conserved between *S. pneumoniae* strains[40] and therefore unlikely to be predictors of serotype. Transport of essential substrates is also achieved by alternative systems which were also captured by our approach, such as the passive channel sodium symporter GlyP[41] or the use of menaquinones and ubiquinones for electron transport (mevalonate pathway)[42–44]. We also found some of the top-scoring entries to be involved in functions associated with respiration (*ecsA, mvaD, mvaK2*) and amino acid, fatty acid and cell wall or capsular biosynthesis which amounted for approximately 25% of the top-scoring genes (*trpF, fabG, lysC, mvaD, mvaK2, ritR, pbp1A, pbpX, mraW* and *mraY*).

High RFA scores for serotype were also found among a number of genes flanking the capsular locus which are involved in antibiotic resistance, such as penicillin-binding protein genes *pbpX* and *pbp1A*, the 16S rRNA cytosine-methyltransferase gene *mraW* and the phospho-N-acetylmuramoyl-pentapeptide-transferase gene *mraY*. Genes involved in resistance to other antibiotics such as tomethicillin, vancomycin, daptomycin (*vra* operon)[45] and the broad-spectrum quinolones family (*patB*)[46–48] were also featured in the top-scoring genes. Also of note were entries linked to direct inter- and intra-species competition, either through factors related to immune escape or warfare. These included genes linked to pneumolysin expression and biofilm formation (*luxS*)[49,50], and production of bacteriocins (*blpH*)[51,52], ammonia (*glmS*)[53] and lysozymes (*lytC*)[54,55].

Several top-scoring genes for SC classification are also key determinants of phenotype

The top-scoring genes predicting SC were discordant to the ones determining serotype and approximately 30% were found to have unknown functions (Table 2). However, we also found several examples of genes whose functions (reviewed in supplementary text) would be expected to be naturally linked with particular phenotypes such as virulence (*sodA, lmb, pdhB, varZ, licA*)[32,33,36,37,56–58] or specific virulence traits such as host-cell adherence (*pclA*)[59] or laminin binding (*lmb*)[39]. Several genes were also found to encode or directly produce proteins or protein-complexes which are highly immunogenic, such as the *groEL*[60–62], *lmb*[39], *carB*[63,64], and *licA*[58,65] genes.

Discussion

Our aim, in this paper, was to test the hypothesis that the stratification of pneumococcal populations into distinct sequence clusters or “lineages” occurred through neutral processes, with serotype diversity being superimposed upon the ensuing “clonal” framework to minimize antigenic interference between lineages. To this end, we applied a Random Forest Algorithm (RFA) to assess the contribution of different genes in determining the serotype or sequence cluster of isolates within a dataset containing 616 whole genomes of *S. pneumoniae* collected in Massachusetts (USA)[8], for each of which we had obtained allelic profiles of 2135 genes of both known and unknown function[17]. By selecting the 2.5% of top RFA scores, we effectively focused on the subset of possibly selected units (genes) which present combinations of alleles that appear statistically more informative than expected at the genome level (see Methods for details). We show that by comparing the genomic localization and function of these top-scoring units (genes), general expectations concerning population structure can be revisited[66], and inferences can be made concerning the evolutionary processes underlying the formation, relationship and maintenance of serotype and sequence cluster (lineage) at the population level.

Reassuringly, genes of the capsular locus (cps) and many of those flanking it achieved high RFA scores in predicting serotype. We also found a preponderance of genes scoring highly for serotype prediction to be associated with key functions that could define unique *metabolic types* that would have diversified in order to avoid direct resource competition, as previously proposed[4,17]. Most of these genes were at a distance of less than 6% of the genome to the cps locus. However, linkage disequilibrium is extremely high in this dataset (Fig S7), regardless of genetic distance (with only a slight increase between loci that are less than 10 genes apart); thus, it was not possible to determine whether these had become segregated through competition or by physical and/or functional associations with this locus.

Genes that were highly informative in predicting lineage (sequence cluster) were entirely distinct from those determining serotype. Contrary to what would be expected from a population structure maintained mostly by neutral processes, around a quarter of these genes co-localized within and around the *groESL* operon (marked with * in Table 2), which encodes the macromolecular machinery for a well-studied protein folding system centred around the chaperone GroEL and co-chaperone GroES[67]. In *Escherichia coli*, approximately 10% of total cytosolic proteins, including 67 essential proteins, have been demonstrated to have stable binding to GroEL, with 50 of these confirmed to depend on *groESL* folding via GroEL-depletion experiments[68]. GroEL is also known to be highly immunogenic in *S. pneumoniae*[61,69], as well as in other bacterial species[62,70,71]. This raises the radically alternative possibility that sequence clustering may have arisen from immune selection operating on groEL in conjunction with extensive coadaptation with genes encoding the proteins which rely on this chaperonin system.

Our results provide a mechanistic basis for the distinction proposed by Croucher and colleagues[7], in the context of the same dataset, between infrequent macroevolutionary changes providing a stable backdrop for more frequent, and often transient, microevolutionary changes (see Figure 3). The differentiation of the *groESL* operon would be a striking example of macroevolution, not only driving the emergence of *S. pneumoniae* sequence clusters but also serving to genealogically distinguish closely related bacterial species[29–31]. Several other genes scoring highly for SC were also found to encode or directly produce proteins or protein-complexes which are highly immunogenic (eg. *lmb, carB, licA*), and these may contribute to the maintenance of lineage structure by co-selection with groEL in accordance with the strain theory of host-pathogen systems in which immune selection operating on multiple immunogenic loci can cause the emergence of non-overlapping combinations of alleles[74–76]. In contrast, the emergence and maintenance of serotypes within major lineages (SC) would be dictated by differentiation in genes within and surrounding the capsular locus, and less permanent associations could arise between SC and serotype (at a microevolutionary scale) through resource competition[14,17] or indeed multi-locus immune selection operating on GroEL, cps, as well as other surface antigens[73].

We note that genes belonging to the Rec family are positioned in close proximity to both the contiguous clusters of top-scoring genes for SC and serotype (Tables 1 and 2). For example, the top-scoring gene *recX* is in close proximity to the *groESL* operon and encodes a regulatory protein that inhibits the RecA recombinase in multiple species of bacteria[77–80]. Restriction-modification systems (RMS) have been proposed as a means of maintaining species identity in a number of bacterial systems[81] and this idea has been extended to the maintenance of lineages within meningococcal[82] and pneumococcal[7] species. Within our framework, RMS would act at even more local scale, principally to conserve the function of critical operons such as

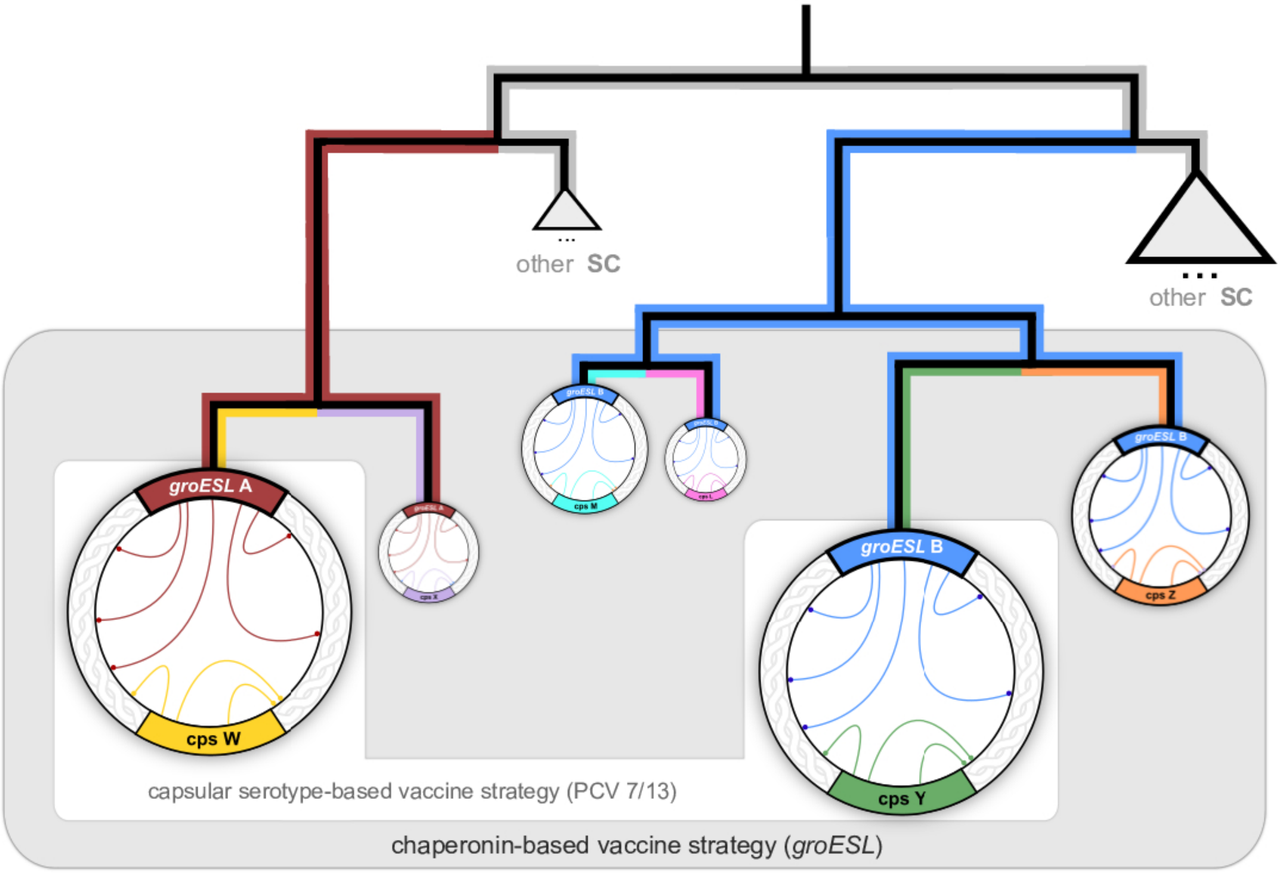

Figure 3. Population structure and vaccination. Conceptual representation of phylogenetic relationships between serotypes and Sequence Clusters (SC), where the former are defined by variation at the cps locus (arbitrarily designated X, W, Y, Z, M, and L, respectively coloured purple, yellow, green, orange, cyan and pink) and the latter are linked to variation in the *groESL* operon (arbitrarily designated A and B and respectively coloured red and blue). Circles symbolize genotypes, with size relative to their prevalence at the population level. Inner genome arcs represent epistatic links: those with the *groESL* operon extend across the genome, while links with the cps locus are more local. Within our framework and according to observed patterns[8], most SCs will be dominantly associated with a single serotype. Current vaccine strategies (white area) that target a selection of capsular serotypes can lead to the expansion of non-vaccine serotypes (VISR,[72,73]), potentially within the same sequence cluster (VIMS[17]). Vaccine strategies based on *groESL* variants (grey area) would target entire SCs instead, including all uncommon serotypes within and thereby preventing their expansion.

groESL, rather than prevent their recombination with other genes or operons. It has recently been demonstrated that GroEL in *E. coli* can be functionally replaced, at least partially, by an eukaryotic chaperonin[83] indicating that the maintenance of particular associations of genes with the *groESL* operon is a consequence of their superior fitness rather than an inability to recombine. We would therefore argue that RMS play a role in protecting the modularity of the genome and that population structure arises through selection favouring particular combinations of variants of these modules.

Overall, our analyses support the hypothesis that lineage structure in maintained by co-adaptation and competition (Buckee et al, 2008) and show, surprisingly, that these selection pressures converge upon the capsular locus and *groESL* operon. Our results endorse the development of vaccines against the associated chaperone protein, groEL, since targetting its protein folding machinery may provide a robust method (Fig. 3) of eliminating particular highly successful lineages rather than promoting the survival of those genotypes within it which carry cps loci encoding non-vaccine capsular serotypes (Watkins et al, 2015). We hope, for these reasons, that this work will stimulate further empirical testing of our hypothesis that immune selection against groEL may be a primary driver of lineage differentiation in the pneumococcus.

Methods

Sequence Data and Allelic Annotation

We used a dataset sequenced by Croucher et al, comprising 616 carriage *S. pneumonaie* genomes isolated in 2001, 2004 and 2007 from Massachusetts (USA). The data included 133, 203, 280 samples from 2001, 2004, 2007, respectively; and is stratified into 16 samples of serotype 10A, 50 of 11A, 7 of 14, 24 of 15A, 60 of 15BC, 8 of 16F, 5 of 17F, 6 of 18C, 73 of 19A, 33 of 19F, 1 of 21, 21 of 22F, 33 of 23A, 23 of 23B, 17 of 23F, 11 of 3, 4 of 31, 5 of 33F, 6 of 34, 49 of 35B, 18 of 35F, 2 of 37, 9 of 38, 47 of 6A, 17 of 6B, 33 of 6C, 3 of 7C, 11 of 7F, 4 of 9N, 6 of 9V and 14 of NT (see[8] for collection details). In summary, we performed a whole genome multi-locus sequence typing (wgMLST) allelic notation[26] using the BIGSdb software with an automated BLAST process[84] and the Genome Comparator tool (with ATCC700669 serotype 23F, accession number FM211187, as the reference genome)[17]. This wgMLST approach resulted in the identification of 2135 genes in common between the reference and all the samples in the dataset. Alleles identical to the reference were classified as '1', with subsequent sequences, differing at least by one base, labelled in increasing order. Genes were further classified as allele 'X' when genetic data present had no match to the genome of interest, or were found to be truncated or non-coding. For a visual representation of the allelic annotation and diversity please refer to S1 dataset of[17]. The allelic matrix as obtained by this approach and used in the RFA analysis is herein made available in supplementary Table S1, which also includes the Accession Numbers, gene name, gene product, gene position in reference genome, and year of collection, Sequence Cluster and serotype of each sample.

Random Forest Approach

We implement a machine learning approach based on a Random Forest Algorithm (RFA) to predict particular features (serotype or Sequence Cluster) of each pneumococci isolate from information on the wgMLST allelic composition of the 2135 genes[85]. In summary, the RFA process takes the following pseudo-steps: (I) the response variable and predictor variables are chosen by the user; (II) a predefined number of independent bootstrap samples are drawn from the dataset with replacement, and a classification tree is fit to each sample containing roughly 2/3 of the data, for which predictor variable selection on each node split in the tree is conducted using only a small random subset of predictor variables; (III) the complete set of trees, one for each bootstrap sample, composes the random forest, from which the status (classification) of the response variable is predicted as an average (majority vote) of the predictions of all trees. Compared to single classification tress, RFs increase prediction accuracy, since the ensemble of slight different classification results adjusts for the instability of the individual trees and avoids data overfitting[86].

Here we use randomForest: Breiman and Cutler's Random Forests for Classification and Regression, a software package for the R-statistical environment[87]. Predictor variables are set to be each gene in our genome samples and the response variable is set to the serotype or Sequence Cluster classification of each genome (as per[8]). We use the Mean Decrease Accuracy (MDA), or Breiman-Cutler importance, as a measure of predictor variable importance, for which classification accuracy after data permutation of a predictor variable is subtracted from the accuracy without permutation, and averaged over all trees in the RF to give an importance value[86]. The strategy herein employed is not of quantitative nature, as the absolute scale of scores produced by the RFA is dependent on the dataset being analyzed[85]. Instead, we focus on the 2.5% of top RFA scores as presented by the resulting MDA distribution for all genes, thus selecting the subset of genes which present combinations of alleles that appear statistically more informative than expected at the genome level (i.e. we assume that 95% of the scores should fall between the 2.5th and 97.5th percentiles). With this assumption and the approach detailed below, we effectively select the genes which present a p-value< 0.05 given an intrinsic distribution of scores generated by data permutation (a null distribution of scores).

For the results presented in the main text, we assume the predictor variables to be numerical (as opposed to categorical). This assumption is known to introduce RF biases, as classification is effectively made by regression and artificial correlations between allele numbering and the features being selected (serotype and Sequence Cluster) may be present. The assumption is herein necessary since the RFA R-based implementation (version 3.6.12) has an upper limit of 53 categories per predictor variable and we find some genes to present up to 6 times this limit in allele diversity. The categorical constraint is a common feature of RFA implementations, as predictor variables with N categories imply 2^N possible (binary) combinations for an internal node split, making the RFA method computationally impractical. Given this inherent RFA limitation, we implemented an input randomization strategy (random reassignment of values to alleles) to minimize potential bias. For this, M random permutations of each gene's allelic numbering in the original dataset is performed, effectively creating M independent input matrices. The RFA is run over the input matrices and in the main results we present each gene's average MDA score. A sensitivity analysis was performed by comparing RFA results between two independent sets of $M = 50$ input matrices (effectively comparing 100 independent runs) (Fig. S5). Results suggest that the existing biases in independent runs of the RFA due to the assumption of numerical predictors are virtually mitigated with our input randomization strategy approach, specially for experiments classifying serotype.

References

1. Song, J. Y. *et al.* Clinical and economic burden of invasive pneumococcal disease in adults: a multicenter hospital-based study. *BMC infectious diseases* **13**, 202 (2013). DOI 10.1186/1471-2334-13-202.
2. O'Brien, K. L. *et al.* Burden of disease caused by Streptococcus pneumoniae in children younger than 5 years: global estimates. *The Lancet* **374**, 893–902 (2009). DOI 10.1016/S0140-6736(09)61204-6.
3. Hausdorff, W. P., Feikin, D. R. & Klugman, K. P. Epidemiological differences among pneumococcal serotypes. *Lancet Infectious Diseases* **5**, 83–93 (2005). DOI 10.1016/S1473-3099(05)01280-6.
4. Cobey, S. & Lipsitch, M. Niche and neutral effects of acquired immunity permit coexistence of pneumococcal serotypes. *Science (New York, N.Y.)* **335**, 1376–80 (2012). DOI 10.1126/science.1215947. NIHMS150003.
5. Maiden, M. C. *et al.* Multilocus sequence typing: a portable approach to the identification of clones within populations of pathogenic microorganisms. *Proceedings of the National Academy of Sciences of the United States of America* **95**, 3140–5 (1998). DOI 10.1073/pnas.95.6.3140.
6. Spratt, B. G. Multilocus sequence typing: Molecular typing of bacterial pathogens in an era of rapid DNA sequencing and the Internet. *Current Opinion in Microbiology* **2**, 312–316 (1999). DOI 10.1016/S1369-5274(99)80054-X.
7. Croucher, N. J. *et al.* Diversification of bacterial genome content through distinct mechanisms over different timescales. *Nature Communications* **5**, 1–12 (2014). DOI 10.1038/ncomms6471.
8. Croucher, N. J. *et al.* Population genomics of post-vaccine changes in pneumococcal epidemiology. *Nature genetics* **45**, 656–63 (2013). DOI 10.1038/ng.2625.
9. Cremers, A. J. H. *et al.* The post-vaccine microevolution of invasive Streptococcus pneumoniae. *Scientific reports* **5**, 14952 (2015). DOI 10.1038/srep14952.
10. Brueggemann, A. *et al.* Clonal Relationships between Invasive and Carriage <i>Streptococcus pneumoniae</i> and Serotype- and Clone-Specific Differences in Invasive Disease Potential. *The Journal of Infectious Diseases* **187**, 1424–1432 (2003). DOI 10.1086/374624.
11. Beall, B. W. *et al.* Shifting genetic structure of invasive serotype 19A pneumococci in the United States. *Journal of Infectious Diseases* **203**, 1360–1368 (2011). DOI 10.1093/infdis/jir052.
12. Henriques-Normark, B., Blomberg, C., Dagerhamn, J., Bättig, P. & Normark, S. The rise and fall of bacterial clones: Streptococcus pneumoniae. *Nature reviews. Microbiology* **6**, 827–37 (2008). DOI 10.1038/nrmicro2011.
13. Fraser, C., Hanage, W. P. & Spratt, B. G. Neutral microepidemic evolution of bacterial pathogens. *Proceedings of the National Academy of Sciences of the United States of America* **102**, 1968–73 (2005). DOI 10.1073/pnas.0406993102.
14. Buckee, C. O. *et al.* Role of selection in the emergence of lineages and the evolution of virulence in Neisseria meningitidis. *Proceedings of the National Academy of Sciences of the United States of America* **105**, 15082–7 (2008). DOI 10.1073/pnas.0712019105.
15. Watkins, E. R., Maiden, M. C. & Gupta, S. Metabolic competition as a driver of bacterial population structure. *Future Microbiology* fmb–2016–0079 (2016). DOI 10.2217/fmb-2016-0079.
16. Bidossi, A. *et al.* A functional genomics approach to establish the complement of carbohydrate transporters in Streptococcus pneumoniae. *PLoS ONE* **7**, e33320 (2012). DOI 10.1371/journal.pone.0033320.
17. Watkins, E. R. *et al.* Vaccination Drives Changes in Metabolic and Virulence Profiles of Streptococcus pneumoniae. *PLoS pathogens* **11**, e1005034 (2015). DOI 10.1371/journal.ppat.1005034.
18. Meng, Y. a., Yu, Y., Cupples, L. A., Farrer, L. a. & Lunetta, K. L. Performance of random forest when SNPs are in linkage disequilibrium. *BMC Bioinformatics* **10**, 78 (2009). DOI 10.1186/1471-2105-10-78.
19. Slabbinck, B., Waegeman, W., Dawyndt, P., De Vos, P. & De Baets, B. From learning taxonomies to phylogenetic learning: integration of 16S rRNA gene data into FAME-based bacterial classification. *BMC bioinformatics* **11**, 69 (2010). DOI 10.1186/1471-2105-11-69.
20. Aguas, R. & Ferguson, N. M. Feature Selection Methods for Identifying Genetic Determinants of Host Species in RNA Viruses. *PLoS Computational Biology* **9** (2013). DOI 10.1371/journal.pcbi.1003254.
21. Eng, C. L. P., Tong, J. C. & Tan, T. W. Predicting host tropism of influenza A virus proteins using random forest. *BMC Medical Genomics* **7**, S1–S1 (2014). DOI 10.1186/1755-8794-7-S3-S1.
22. Eng, C. L. P., Tong, J. C. & Tan, T. W. Distinct host tropism protein signatures to identify possible zoonotic influenza a viruses. *PLoS ONE* **11**, 1–12 (2016). DOI 10.1371/journal.pone.0150173.

23. Lupolova, N., Dallman, T. J., Matthews, L., Bono, J. L. & Gally, D. L. Support vector machine applied to predict the zoonotic potential of <i>E. coli</i> O157 cattle isolates. *Proceedings of the National Academy of Sciences* 201606567 (2016). DOI 10.1073/pnas.1606567113.

24. Alam, M. T. *et al.* Dissecting vancomycin-intermediate resistance in staphylococcus aureus using genome-wide association. *Genome Biology and Evolution* **6**, 1174–1185 (2014). DOI 10.1093/gbe/evu092.

25. Burstein, D. *et al.* Genomic analysis of 38 Legionella species identifies large and diverse effector repertoires. *Nature Genetics* **48**, 167–175 (2016). DOI 10.1038/ng.3481.

26. Klemm, E. & Dougan, G. Advances in Understanding Bacterial Pathogenesis Gained from Whole-Genome Sequencing and Phylogenetics. *Cell Host and Microbe* **19**, 599–610 (2016). DOI 10.1016/j.chom.2016.04.015.

27. Austerlitz, F. *et al.* DNA barcode analysis: a comparison of phylogenetic and statistical classification methods. *BMC bioinformatics* **10 Suppl 1**, S10 (2009). DOI 10.1186/1471-2105-10-S14-S10.

28. Bentley, S. D. *et al.* Putatively novel serotypes and the potential for reduced vaccine effectiveness: capsular locus diversity revealed among 5,405 pneumococcal genomes. *Microbial Genomics* **2** (2016). DOI 10.1099/mgen.0.000090.

29. Glazunova, O. O., Raoult, D. & Roux, V. Partial sequence comparison of the rpoB, sodA, groEL and gyrB genes within the genus Streptococcus. *International Journal of Systematic and Evolutionary Microbiology* **59**, 2317–2322 (2009). DOI 10.1099/ijs.0.005488-0.

30. Teng, L.-j. *et al.* groESL Sequence Determination , Phylogenetic Analysis , and Species Differentiation for Viridans Group Streptococci groESL Sequence Determination , Phylogenetic Analysis , and Species Differentiation for Viridans Group Streptococci. *Journal of Clinical Microbiology* **40**, 3172–3178 (2002). DOI 10.1128/JCM.40.9.3172.

31. Hung, W. C., Tsai, J. C., Hsueh, P. R., Chia, J. S. & Teng, L. J. Species identification of mutans streptococci by groESL gene sequence. *Journal of Medical Microbiology* **54**, 857–862 (2005). DOI 10.1099/jmm.0.46180-0.

32. Obregón, V. *et al.* Molecular peculiarities of the lytA gene isolated from clinical pneumococcal strains that are bile insoluble. *Journal of Clinical Microbiology* **40**, 2545–2554 (2002). DOI 10.1128/JCM.40.7.2545-2554.2002.

33. Arbique, J. C. *et al.* Accuracy of phenotypic and genotypic testing for identification of Streptococcus pneumoniae and description of Streptococcus pseudopneumoniae sp. nov. *Journal of Clinical Microbiology* **42**, 4686–4696 (2004). DOI 10.1128/JCM.42.10.4686-4696.2004.

34. Poyart, C., Quesne, G., Coulon, S., Berche, P. & Trieu-Cuot, P. Identification of streptococci to species level by sequencing the gene encoding the manganese-dependent superoxide dismutase. *Journal of Clinical Microbiology* **36**, 41–47 (1998).

35. Martín-Galiano, A. J., Balsalobre, L., Fenoll, A. & De la Campa, A. G. Genetic characterization of optochin-susceptible viridans group streptococci. *Antimicrobial Agents and Chemotherapy* **47**, 3187–3194 (2003). DOI 10.1128/AAC.47.10.3187-3194.2003.

36. Spellerberg, B. *et al.* Lmb, a protein with similarities to the LraI adhesin family, mediates attachment of Streptococcus agalactiae to human laminin. *Infection and Immunity* **67**, 871–878 (1999).

37. Terao, Y., Kawabata, S., Kunitomo, E., Nakagawa, I. & Hamada, S. Novel laminin-binding protein of Streptococcus pyogenes, Lbp, is involved in adhesion to epithelial cells. *Infection and Immunity* **70**, 993–997 (2002). DOI 10.1128/IAI.70.2.993.

38. Zhang, Y. M. *et al.* Prevalent distribution and conservation of streptococcus suis lmb protein and its protective capacity against the chinese highly virulent strain infection. *Microbiological Research* **169**, 395–401 (2014). DOI 10.1016/j.micres.2013.09.007.

39. Wahid, R. M. *et al.* Immune response to a laminin-binding protein (Lmb) in group a streptococcal infection. *Pediatrics International* **47**, 196–202 (2005). DOI 10.1111/j.1442-200x.2005.02038.x.

40. Jomaa, M. *et al.* Immunization with the iron uptake ABC transporter proteins PiaA and PiuA prevents respiratory infection with Streptococcus pneumoniae. *Vaccine* **24**, 5133–5139 (2006). DOI 10.1016/j.vaccine.2006.04.012.

41. Reizer, J., Reizer, A. & Saier, M. H. A functional superfamily of sodium/solute symporters. *Biochimica et biophysica acta* **1197**, 133–66 (1994). DOI 10.1016/0304-4157(94)90003-5.

42. Wilding, E. I. *et al.* Identification, essentiality and evolution of the mevalonate pathway for isopentenyl diphosphate biosynthesis in {Gram}-positive cocci. *J. Bacteriology* **182**, 4319–4327 (2000). DOI 10.1128/JB.182.15.4319-4327.2000.Updated.

43. Buhaescu, I. & Izzedine, H. Mevalonate pathway: A review of clinical and therapeutical implications. *Clinical Biochemistry* **40**, 575–584 (2007). DOI 10.1016/j.clinbiochem.2007.03.016.

44. Holstein, S. A. & Hohl, R. J. Isoprenoids: Remarkable diversity of form and function. *Lipids* **39**, 293–309 (2004). DOI 10.1007/s11745-004-1233-3.

45. Boyle-Vavra, S., Yin, S., Jo, D. S., Montgomery, C. P. & Daum, R. S. VraT/YvqF is required for methicillin resistance and activation of the VraSR regulon in Staphylococcus aureus. *Antimicrobial Agents and Chemotherapy* **57**, 83–95 (2013). DOI 10.1128/AAC.01651-12.

46. Garvey, M. I., Baylay, A. J., Wong, R. L. & Piddock, L. J. V. Overexpression of patA and patB, which encode ABC transporters, is associated with fluoroquinolone resistance in clinical isolates of Streptococcus pneumoniae. *Antimicrobial Agents and Chemotherapy* **55**, 190–196 (2011). DOI 10.1128/AAC.00672-10.

47. El Garch, F. *et al.* Fluoroquinolones induce the expression of patA and patB, which encode ABC efflux pumps in Streptococcus pneumoniae. *Journal of Antimicrobial Chemotherapy* **65**, 2076–2082 (2010). DOI 10.1093/jac/dkq287.

48. Boncoeur, E. *et al.* PatA and PatB form a functional heterodimeric ABC multidrug efflux transporter responsible for the resistance of streptococcus pneumoniae to fluoroquinolones. *Biochemistry* **51**, 7755–7765 (2012). DOI 10.1021/bi300762p.

49. Joyce, E. A. *et al.* LuxS Is Required for Persistent Pneumococcal Carriage and Expression of Virulence and Biosynthesis Genes. *Infection and Immunity* **72**, 2964–2975 (2004). DOI 10.1128/IAI.72.5.2964-2975.2004.

50. Xu, L. *et al.* Role of the luxS Quorum-Sensing System in Biofilm Formation and Virulence of Staphylococcus epidermidis Role of the luxS Quorum-Sensing System in Biofilm Formation and Virulence of Staphylococcus epidermidis. *Infection and immunity* **74**, 488–496 (2006). DOI 10.1128/IAI.74.1.488.

51. De Saizieu, A. *et al.* Microarray-based identification of a novel Streptococcus pneumoniae regulon controlled by an autoinduced peptide. *Journal of Bacteriology* **182**, 4696–4703 (2000). DOI 10.1128/JB.182.17.4696-4703.2000.

52. Reichmann, P. & Hakenbeck, R. Allelic variation in a peptide-inducible two-component system of Streptococcus pneumoniae. *FEMS Microbiology Letters* **190**, 231–236 (2000). DOI 10.1016/S0378-1097(00)00340-2.

53. Moye, Z. D., Burne, R. A. & Zeng, L. Uptake and metabolism of N-acetylglucosamine and glucosamine by Streptococcus mutans. *Applied and Environmental Microbiology* **80**, 5053–5067 (2014). DOI 10.1128/AEM.00820-14.

54. García, P., González, M. P., García, E., García, J. L. & López, R. The molecular characterization of the first autolytic lysozyme of Streptococcus pneumoniae reveals evolutionary mobile domains. *Molecular Microbiology* **33**, 128–138 (1999). DOI 10.1046/j.1365-2958.1999.01455.x.

55. Eldholm, V., Johnsborg, O., Haugen, K., Ohnstad, H. S. & Havastein, L. S. Fratricide in Streptococcus pneumoniae: Contributions and role of the cell wall hydrolases CbpD, LytA and LytC. *Microbiology* **155**, 2223–2234 (2009). DOI 10.1099/mic.0.026328-0.

56. Iacobone, M., Mantero, F., Basso, S. M., Lumachi, F. & Favia, G. Results and long-term follow-up after unilateral adrenalectomy for ACTH-independent hypercortisolism in a series of fifty patients. *Journal of Endocrinological Investigation* **28**, 327–332 (2005). DOI 3106 [pii].

57. Pancholi, V. & Chhatwal, G. S. Housekeeping enzymes as virulence factors for pathogens. *International Journal of Medical Microbiology* **293**, 391–401 (2003). DOI 10.1078/1438-4221-00283.

58. Humphries, H. E. & High, N. J. The role of licA phase variation in the pathogenesis of invasive disease by Haemophilus influenzae type b. *FEMS Immunology and Medical Microbiology* **34**, 221–230 (2002). DOI 10.1016/S0928-8244(02)00394-2.

59. Paterson, G. K., Nieminen, L., Jefferies, J. M. C. & Mitchell, T. J. PclA, a pneumococcal collagen-like protein with selected strain distribution, contributes to adherence and invasion of host cells. *FEMS Microbiology Letters* **285**, 170–176 (2008). DOI 10.1111/j.1574-6968.2008.01217.x.

60. Kim, S. N., Kim, S. W., Pyo, S. N. & Rhee, D. K. Molecular cloning and characterization of groESL operon in Streptococcus pneumoniae. *Mol Cells* **11**, 360–368 (2001).

61. Cao, J. *et al.* Protection against pneumococcal infection elicited by immunization with multiple pneumococcal heat shock proteins. *Vaccine* **31**, 3564–3571 (2013). DOI 10.1016/j.vaccine.2013.05.061.

62. Péchiné, S., Hennequin, C., Boursier, C., Hoys, S. & Collignon, A. Immunization using GroEL decreases Clostridium difficile intestinal colonization. *PLoS ONE* **8** (2013). DOI 10.1371/journal.pone.0081112.

63. Svenson, S. B. & Lindberg, A. L. F. A. Artificial Salmonella Vaccines : Salmonella typhimurium 0- Antigen-Specific Oligosaccharide-Protein Conjugates Elicit Protective Antibodies in Rabbits and Mice **32**, 490–496 (1981).

64. Kalynych, S., Morona, R. & Cygler, M. Progress in understanding the assembly process of bacterial O-antigen. *FEMS Microbiology Reviews* **38**, 1048–1065 (2014). DOI 10.1111/1574-6976.12070.

65. Serino, L. & Virji, M. Phosphorylcholine decoration of lipopolysaccharide differentiates commensal Neisseriae from pathogenic strains: Identification of licA-type genes in commensal Neisseriae. *Molecular Microbiology* **35**, 1550–1559 (2000). DOI 10.1046/j.1365-2958.2000.01825.x.

66. McInerney, J. O. More than tree dimensions: Inter-lineage evolution's ecological importance. *Trends in Ecology and Evolution* **28**, 924–625 (2013). DOI 10.1016/j.tree.2013.09.002.

67. Hayer-Hartl, M., Bracher, A. & Hartl, F. U. The GroEL-GroES Chaperonin Machine: A Nano-Cage for Protein Folding (2016).

68. Kerner, M. J. *et al.* Proteome-wide analysis of chaperonin-dependent protein folding in Escherichia coli. *Cell* **122**, 209–220 (2005). DOI 10.1016/j.cell.2005.05.028.

69. Khan, M. N., Shukla, D., Bansal, A., Mustoori, S. & Ilavazhagan, G. Immunogenicity and protective efficacy of GroEL (hsp60) of Streptococcus pneumoniae against lethal infection in mice. *FEMS Immunology and Medical Microbiology* **56**, 56–62 (2009). DOI 10.1111/j.1574-695X.2009.00548.x.

70. Hennequin, C. *et al.* GroEL (Hsp60) of Clostridium difficile is involved in cell adherence. *Microbiology* **147**, 87–96 (2001). DOI 10.1099/00221287-147-1-87.

71. Wuppermann, F. N., Mölleken, K., Julien, M., Jantos, C. A. & Hegemann, J. H. Chlamydia pneumoniae GroEL1 protein is cell surface associated and required for infection of HEp-2 cells. *Journal of Bacteriology* **190**, 3757–3767 (2008). DOI 10.1128/JB.01638-07.

72. Chang, Q. *et al.* Stability of the pneumococcal population structure in Massachusetts as PCV13 was introduced. *BMC infectious diseases* **15**, 68 (2015). DOI 10.1186/s12879-015-0797-z.

73. Croucher, N. J. *et al.* Selective and Genetic Constraints on Pneumococcal Serotype Switching. *PLoS Genetics* **11**, 1–21 (2015). DOI 10.1371/journal.pgen.1005095.

74. Gupta, S. Chaos, Persistence, and Evolution of Strain Structure in Antigenically Diverse Infectious Agents. *Science* **280**, 912–915 (1998). DOI 10.1126/science.280.5365.912.

75. Gupta, S. *et al.* The maintenance of strain structure in populations of recombining infectious agents. *Nature medicine* **2**, 437–42 (1996). DOI 10.1038/nm0496-437.

76. Lourenço, J., Wikramaratna, P. S. & Gupta, S. MANTIS: an R package that simulates multilocus models of pathogen evolution. *BMC bioinformatics* **16**, 176 (2015). DOI 10.1186/s12859-015-0598-9.

77. Bergé, M., Mortier-Barrière, I., Martin, B. & Claverys, J. P. Transformation of Streptococcus pneumoniae relies on DprA- and RecA-dependent protection of incoming DNA single strands. *Molecular Microbiology* **50**, 527–536 (2003). DOI 10.1046/j.1365-2958.2003.03702.x.

78. Venkatesh, R. *et al.* RecX protein abrogates ATP hydrolysis and strand exchange promoted by RecA: insights into negative regulation of homologous recombination. *Proceedings of the National Academy of Sciences of the United States of America* **99**, 12091–12096 (2002). DOI 10.1073/pnas.192178999.

79. Stohl, E. A. *et al.* Escherichia coli RecX inhibits RecA recombinase and coprotease activities in vitro and in vivo. *Journal of Biological Chemistry* **278**, 2278–2285 (2003). DOI 10.1074/jbc.M210496200.

80. Galvão, C. W. *et al.* The RecX protein interacts with the RecA protein and modulates its activity in herbaspirillum seropedicae. *Brazilian Journal of Medical and Biological Research* **45**, 1127–1134 (2012). DOI 10.1590/S0100-879X2012007500160.

81. Jeltsch, A. Maintenance of species identity and controlling speciation of bacteria: A new function for restriction/modification systems? *Gene* **317**, 13–16 (2003). DOI 10.1016/S0378-1119(03)00652-8.

82. Budroni, S. *et al.* Neisseria meningitidis is structured in clades associated with restriction modification systems that modulate homologous recombination. *Proceedings of the National Academy of Sciences of the United States of America* **108**, 4494–9 (2011). DOI 10.1073/pnas.1019751108. arXiv:1408.1149.

83. Shah, R. *et al.* Replacement of GroEL in Escherichia coli by the Group II Chaperonin from the Archaeon Methanococcus maripaludis. *Journal of Bacteriology* **198**, 2692–2700 (2016). DOI 10.1128/JB.00317-16.

84. Altschul, S., Gish, W., Miller, W., Myers, E. & Lipman, D. Basic local alignment search tool. *Journal of Molecular Biology* **215**, 403–410 (1990). DOI 10.1016/S0022-2836(05)80360-2.

85. Breiman, L. Random forests. *Machine Learning* **45**, 5–32 (2001). DOI 10.1023/A:1010933404324. /dx.doi.org/10.1023{%}2FA{%}3A1010933404324.

86. Friedman, J., Hastie, T. & Tibshirani, R. *No Title* (Berlin: Springer series in statistics, 2001), first edit edn.

87. Liaw, a. & Wiener, M. Classification and Regression by randomForest. *R news* **2**, 18–22 (2002). DOI 10.1177/154405910408300516. 1609-3631.

Acknowledgements

The authors acknowledge the sequence data kindly given by Angela Brueggemann and Andries van Tonder, and Richard Moxon for the valuable comments on a previous version of this manuscript.

Additional Information

The authors declare no competing interests.

Author contributions statement

This research was funded by the European Research Council under the European Union’s Seventh Framework Programme (FP7/2007-2013) / ERC grant agreement no. 268904 - DIVERSITY (www.erc.europa.eu; www.royalsociety.org). The funders had no role in study design, data collection and analysis, decision to publish, or preparation of the manuscript. JL and SG designed the study. JL performed the experiments and wrote the initial manuscript. JL, EWR, SG and MCJM revised the manuscript. JL, UO, SJP and CM curated the data and revised gene functionality.

Supplementary Material

Supplementary Figures S1-7 described in a separate PDF file. The dataset herein used, in the format of an allelic matrix is made available in Table S1 in a separate spreadsheet. Functional description and literature review of top-scoring genes mentioned in the main text are in supplementary text within a separate PDF file.

SPNF23		**Name**	**Type / Function**
00400			Hypothetical protein
02300	a	pitA	Ferric iron ABC transporter, permease protein
02320	a	pitB	Ferric iron ABC transporter, ATP-binding protein
02540	b	glmS	Glucosamine-frutose-6-phosphate aminotransferase
02550	b		Luciferase-like monooxygenase / Oxidoreductase
02560	b	spuA	Surface-anchored pullulanase
02600		polC	DNA polymerase III PolC-type
02870	c		Maltodextrin glucosidase
02880	c	basA	Glutathione peroxidase family protein
03060 *	d	mraW	16S rRNA cytosine-methyltransferase
03070 *	d	ftsL	Cell division protein
03080 *	d	pbpX	Penicillin binding protein / cell division protein
03090 *	d	mraY	Phospho-N-acetylmuramoyl-pentapeptide-transferase
03110 *	d	clpL	ATP-dependent Clp proteinase
03130 *	d	luxS	S-ribosylhomocysteinase lyase
03140 *	d		ATP-dependent Zinc protease
03150 *	d	dexB	Glucan-1 6-alpha-glucosidase
03390 *	e	aliA	Oligopeptide ABC transporter
03410 *	e	pbp1A	Transpeptidase / Penicillin-binding protein
03420 *	e	recU	Holliday junction resolvase
03430 *	e		Hypothetical protein
03450 *	e		23S rRNA / guanine-methyltransferase
03470 *	e	gnd	6-phosphogluconate dehydrogenase
03480 *	e	ritR	Response regulator
03540	f	mvaD	Mevalonate diphosphate decarboxylase
03550	f	mvaK2	Mevalonate kinase
03560	f	fni	Isopentenyl-diphosphate delta-isomerase
03570	f	vraT	Cell wall-active antibiotics response protein
03580	f	vraS	Sensor histidine kinase
03840	g	glyP	Sodium glycine symporter
03860	g	shetA	Exfoliative toxin
03870	g	serS	Seryl-tRNA synthetase
03890	g	lysC	Aspartokinase
03960		fabG	3-oxoacyl-acyl-carrier protein reductase
04740	h	ecsA	ABC transporter ATP-binding protein
04790	h	blpH	Histidine kinase of the competence regulon ComD
15900		lytC	Glucan-binding domain / Lysozyme M1
18330		trpF	Phosphoribosylanthranilate isomerase
20980		patB	Multidrug resistance ABC transporter

Table 1. Top genes for Serotype prediction. Genes marked with * flank up to 10 genes, upstream or downstream from the capsular locus. Letters *a* to *h* denote groups of contiguous genes (minimum proximity of 2 genes).

SPNF23		**Name**	**Type / Function**
00090			Phospholycenate mutase
00540		recO	DNA recombination and repair protein
00660		vanZ	Teicoplanin resistance protein
02370			Transcriptional regulator
03790		spi	Signal peptidase I
04050			Hypothetical protein
04730			Histidine triad nucleotide-binding protein
06210			ABC transporter, ATP-binding protein
06880		sodA	Manganese superoxide dismutase
07240			Hypothetical protein
07340			Hydrolase / Haloacid dehalogenase-like family
07930		iscU	Putative iron-sulfur cluster assembly scaffold protein
08320			Putative membrane protein
09040			O-methyltransferase family protein C1
09280		lmb	Laminin-binding protein
09460			N-acetyltransferase GNAT family protein
10040			Cytosolic protein containing multiple CBS domains
10480			Hypothetical protein
10670		pdhB	Acetoin dehydrogenase E1 component β-subunit
11320			Acetyltransferase GNAT family protein
11630		licA	Choline kinase
11660		carB	Membrane protein / O-antigen and teichoic acid
13490			Hypothetical protein
14640		lta	Bacterocin transport accessory protein
15100		pclA	Putative NADPH-dependent FMN reductase
16930			Hypothetical protein
17080			Hypothetical protein
18130			Hypothetical protein
19240 *	a	recX	Regulatory protein
19250 *	a		Cysteinyl-tRNA synthase related protein
19300 *	b	groEL	Heat shock protein 60 family chaperone
19310 *	b	groES	Heat shock protein 60 family co-chaperone
19330 *	b		Short-chain dehydrogenase
19340 *	b	ytpR	Phenylalanyl-tRNA synthetase domain protein
19360 *	b		Hypothetical protein
19370 *	b		Hypothetical protein
19380 *	b		Membrane protein
19390 *	b		Response regulator of LytR/AlgR family
20880	c		Hydrolase, haloacid dehalogenase-like family
20900	c	thrC	Threonine synthase
22500		mreD	Rod shape-determining protein

Table 2. Top genes for Sequence Cluster prediction. Genes marked with * flank up to 10 genes, upstream or downstream from the *groESL* operon. Letters *a* to *c* denote groups of contiguous genes (minimum proximity of 2 genes).

(A)
Serotype Classification
Genome position (x 1e+05)
0
5
10
15
20
RFA MDA Score (normalized)
0
0.2
0.4
0.6
0.8
1
(B)
Sequence Cluster Classification
Genome position (x 1e+05)
0
5
10
15
20
RFA MDA Score (normalized)
0
0.2
0.4
0.6
0.8
1

(A)
Serotype Classification
(B)
Sequence Cluster Classification
Genome position (x 1e+05)
0
5
10
15
20
RFA MDA Score (normalized)
0
0.2
0.4
0.6
0.8
1

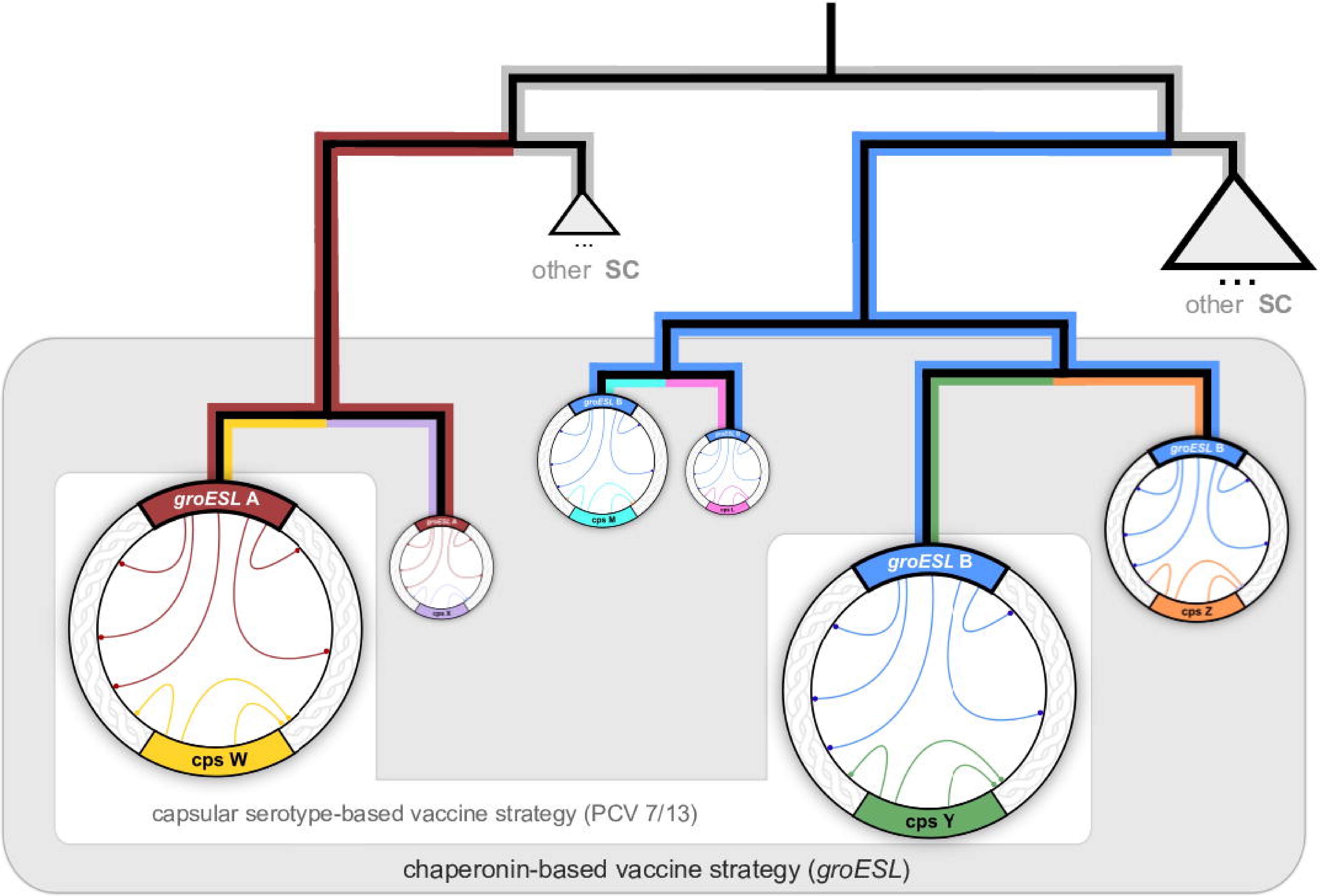other SC
other SC
groESL A
cps W
groESL A
cps X
groESL B
cps M
groESL B
cps L
groESL B
cps Y
groESL B
cps Z
capsular serotype-based vaccine strategy (PCV 7/13)
chaperonin-based vaccine strategy (groESL)